Supplementary Information

S2-peptide conjugated SpyCatcher-Ferritin Nanoparticles elicit broad protection against SARS-CoV-2 variants of concern

Chang-Kyu Heo1, Seonyeong Oh1, Won-Hee Lim1, Jihyun Yang1, Sang Jick Kim2, Euijeon Woo3, Hwi Won Seo1, Eun-Wie Cho1*

1Infectious Disease Research Center, Korea Research Institute of Bioscience and Biotechnology (KRIBB), 125 Gwahak-ro, Yuseong-gu, Daejeon 34141, Republic of Korea.

2Synthetic Biology and Bioengineering Research Center, Korea Research Institute of Bioscience and Biotechnology (KRIBB), 125 Gwahak-ro, Yuseong-gu, Daejeon, 34141, Republic of Korea.

3Bio-design & Editing Research Center, Korea Research Institute of Bioscience and Biotechnology (KRIBB), 125 Gwahak-ro, Yuseong-gu, Daejeon, 34141, Republic of Korea

*Corresponding author: Eun-Wie Cho. E-mail: ewcho@kribb.re.kr

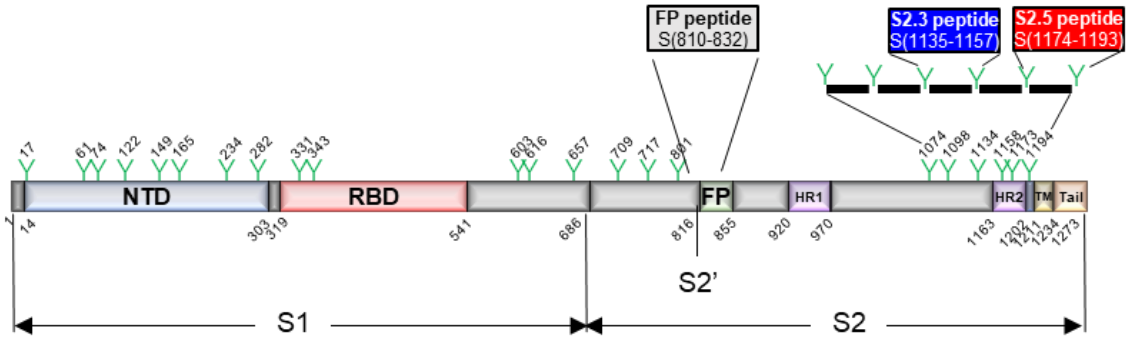

Figure S1. Domain Organization of SARS-CoV-2 Spike Protein and S2 Epitope Mapping.
Schematic representation of the SARS-CoV-2 spike (S) protein and the location of peptide epitopes analyzed in this study. The linear domain organization includes S1 and S2 subunits, receptor-binding domain (RBD), S1/S2 and S2′ cleavage sites, fusion peptide (FP), heptad repeat regions (HR1 and HR2), transmembrane (TM) domain, and cytoplasmic tail (CT). N-linked glycosylation sites are indicated along the sequence. The S2-derived peptide epitopes (S2.3, S2.5, and FP) are highlighted with colored bars, with corresponding amino acid sequences and residue positions indicated. These epitopes map to conserved regions within the S2 subunit.

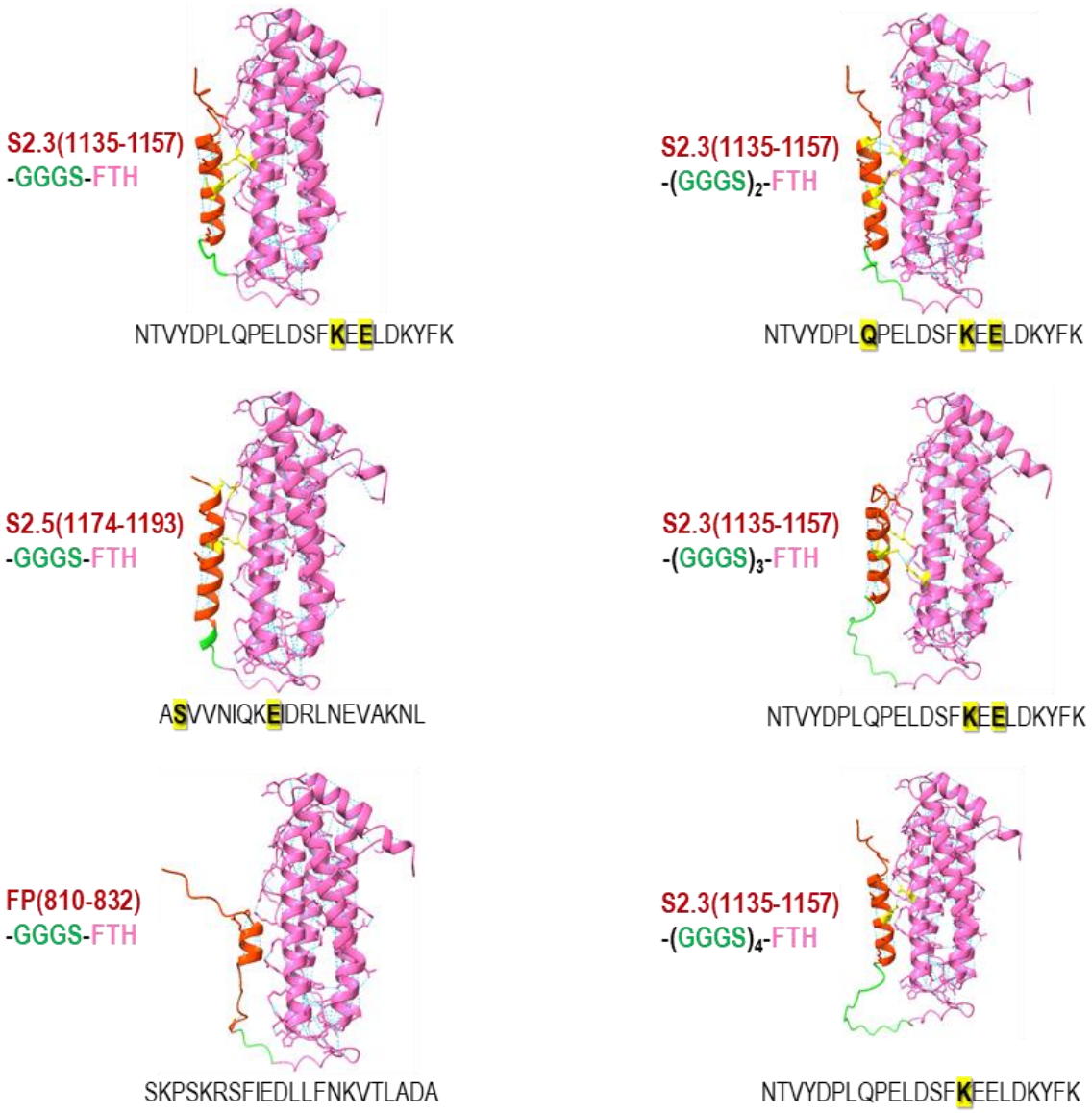

Figure S2. Structural Prediction of S2 Peptide–Ferritin Fusion via Flexible Linkers.

Structural models of S2 peptides (S2.3, S2.5, and fusion peptide [FP]) genetically fused to the N-terminus of ferritin via flexible GGGS linkers (1–4 repeats) were predicted using AlphaFold3. In the models, S2 peptides are shown in red, GGGS linkers in green, and the ferritin subunit in pink. The predicted structures indicate that, regardless of linker length, S2 peptides adopt conformations positioned in close proximity to the ferritin surface. Residues within the S2 peptides that are proximal to the ferritin surface and potentially involved in hydrogen bonding are highlighted in yellow. Corresponding S2 peptide sequences are shown below each model.

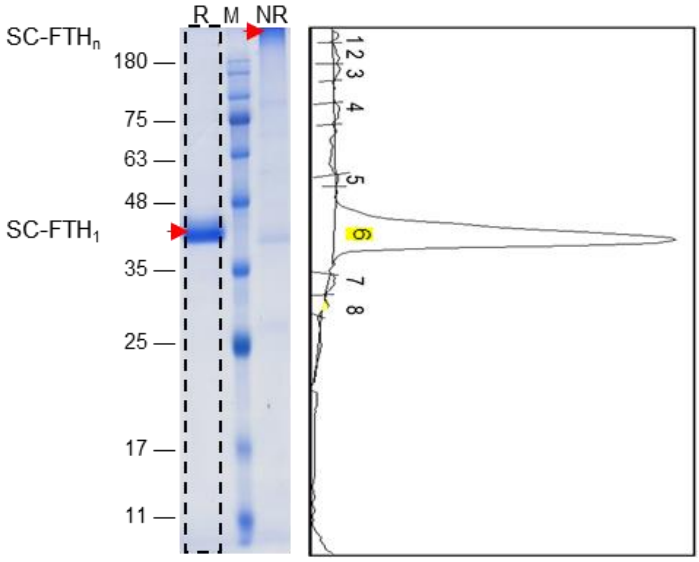

peak	Intensity	%
1	42.657	0.514819
2	79.778	0.962825
3	69.778	0.842137
4	76.364	0.921622
5	18.121	0.218699
6	7863.326	94.90097
7	94.021	1.134721
8	41.778	0.504211
Total	8285.823	100

Figure S3. SDS–PAGE Analysis and Purity Assessment of SC–FTH Nanoparticles.

Purified SC–FTH was analyzed by 12% SDS–PAGE under reducing conditions to assess protein purity. The region indicated by the dashed box in the full gel was used for quantitative analysis. Protein band intensities were quantified by densitometric analysis using ImageJ. The integrated intensity of the SC–FTH band was calculated as a percentage of the total lane intensity to estimate relative purity.

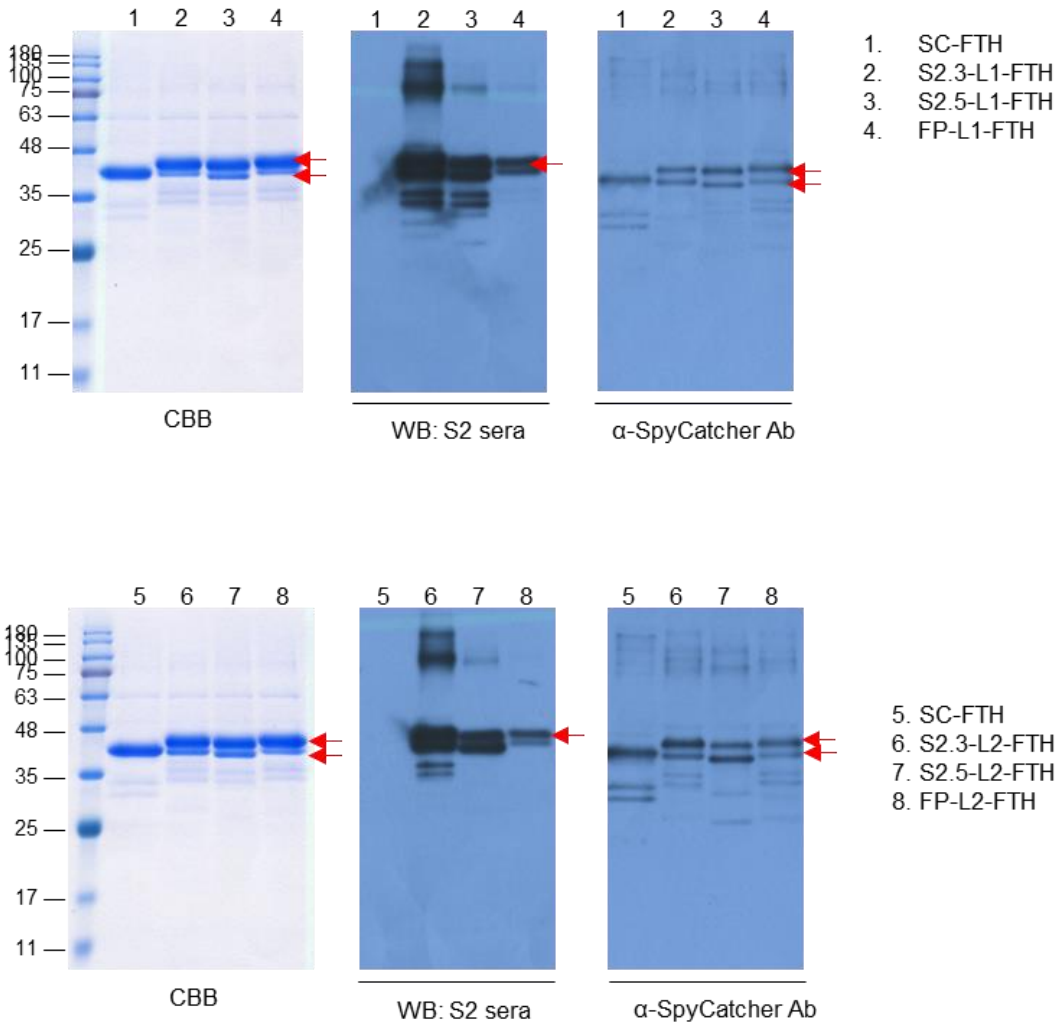

Figure S4. Verification of SpyTag-Mediated Conjugation of S2 Peptides to SC–FTH.

SC–FTH nanoparticles were reacted with SpyTag-fused S2 peptides (S2.3, S2.5, and fusion peptide [FP]) containing variable linker lengths (L1 or L2). Reaction products were analyzed by 12% SDS–PAGE under reducing conditions and visualized by Coomassie Brilliant Blue staining. A mobility shift toward higher molecular weight following conjugation indicates successful SpyCatcher–SpyTag–mediated ligation. Conjugation was further confirmed by Western blot using anti-S2 immune sera or anti-SpyCatcher antibodies, demonstrating the presence of S2 epitopes on SC–FTH conjugates. For each lane, 2 μg of protein was loaded for Coomassie staining and 100 ng for Western blot analysis.

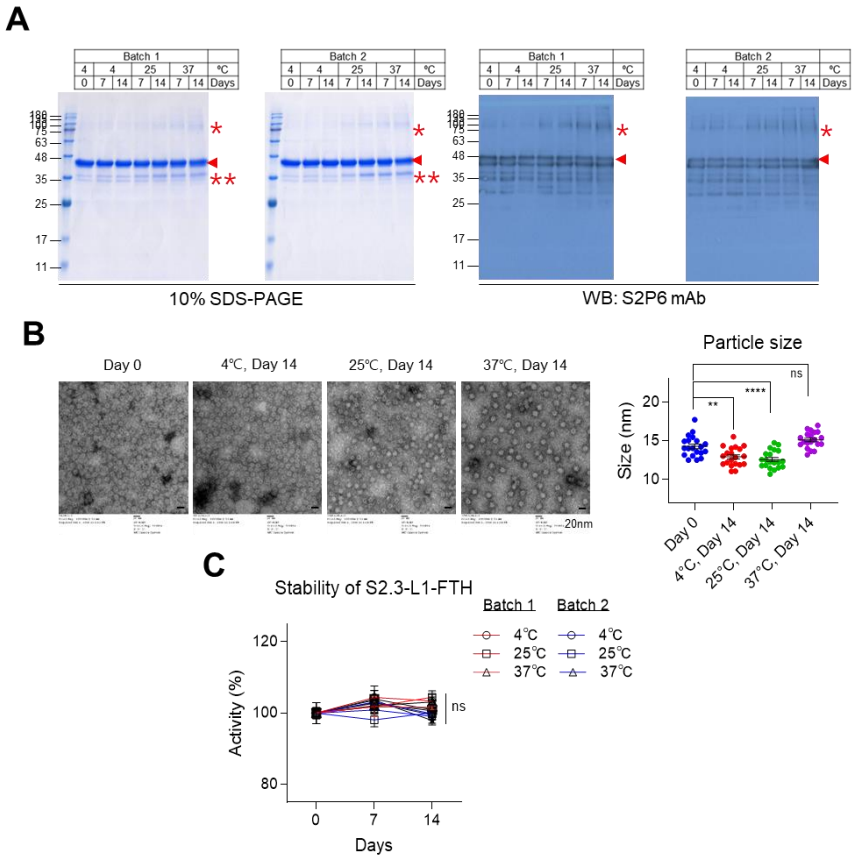

Figure S5. Thermal Stability of S2.3–L1–FTH Nanoparticles.

The thermal stability of the ferritin-based nanovaccine was evaluated using the S2.3–L1–FTH construct after storage at 4 °C, 25 °C, or 37 °C for up to 14 days. S2.3–L1–FTH nanoparticles were prepared in two independent batches, stored under each condition, and sampled at the indicated time points for analysis. **(A)** SDS–PAGE and Western blot analysis using the S2P6 monoclonal antibody to assess protein integrity and retention of the S2.3 epitope following thermal incubation. Bands marked with asterisks (**) increased after storage at 37 °C; however, S2P6-reactive bands of low molecular weight did not increase, suggesting that these bands unlikely to represent degradation products of S2.3–L1–FTH. **(B)** TEM analysis of S2.3–L1–FTH nanoparticles after storage at the indicated temperatures and time points. Scale bar=20nm. Particle size distribution analysis showed minor variations (approximately ±5 nm) depending on storage conditions; however, no evidence of structural disruption, aggregation, or fragmentation was observed, indicating preservation of nanoparticle integrity. **(C)** ELISA analysis of thermally incubated samples using the S2P6 antibody to evaluate the preservation of epitope-specific binding activity relative to day 0 controls. S2.3-coated L1–FTH nanoparticles (30 ng/well) and S2P6 antibody (0.37 ng/well) were used to achieve submaximal binding conditions. Relative binding activity was calculated by normalizing the signal to those obtained from day 0 (4ºC) sample. Statistical significance was assessed by one-way ANOVA ($^{**}p < 0.01$, $^{****}p < 0.0001$; ns, not significant).

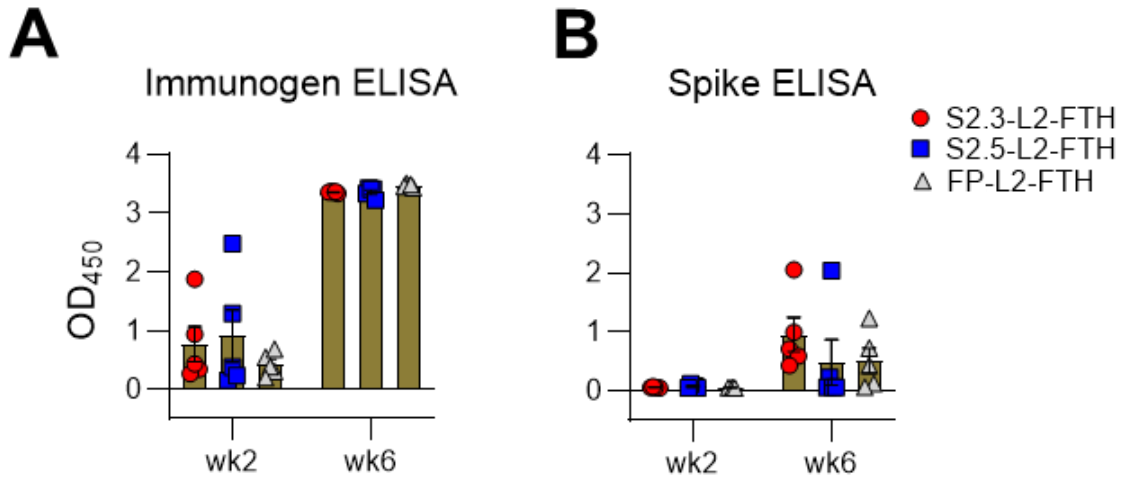

Figure S6. ELISA Analysis of Antibody Responses Induced by L2-Linker Nanoparticles.

ELISA analysis of sera collected at weeks 2 and 6 from mice immunized with S2 peptide–SC-FTH nanoparticles containing two miniPEG2 linkers (L2; S2.3, S2.5, and FP). (A) Antibody responses against the corresponding nanoparticle immunogens. (B) Binding to recombinant spike protein. Data are presented as mean ± SEM (n = 5), with measurements performed in duplicate.

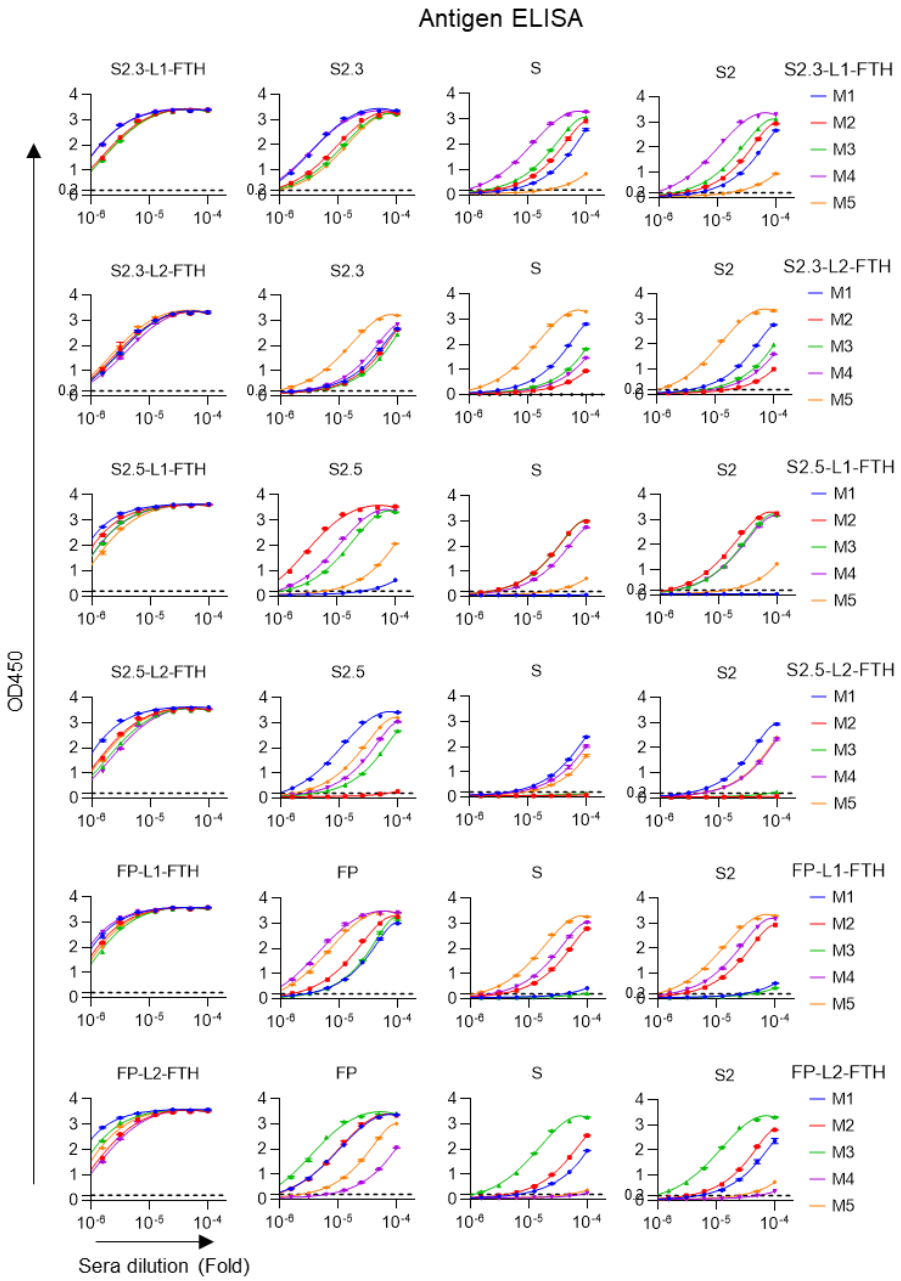

Figure S7. ELISA Binding Curves of Week 11 Antisera to S2 Epitope–Containing Antigens.

Sera collected at week 11 from mice immunized with S2.3–, S2.5–, or FP–FTH nanoparticles containing one or two miniPEG2 linkers (L1 or L2) were analyzed by ELISA. Binding was evaluated against the corresponding immunogens, S2 peptide–BSA conjugates, recombinant S2 protein, and full-length spike protein. Sera were serially diluted from 1:10,000 to 1:1,280,000 in two-fold increments. Raw binding curves used for endpoint titer determination are shown. Each symbol represents an individual mouse (n = 5), and bars indicate mean ± SEM. Endpoint titers were calculated by fitting background-corrected OD values to a four-parameter logistic (4-PL) model and defined as the reciprocal dilution corresponding to the cut-off (mean of negative controls + 3 SD; dashed line).

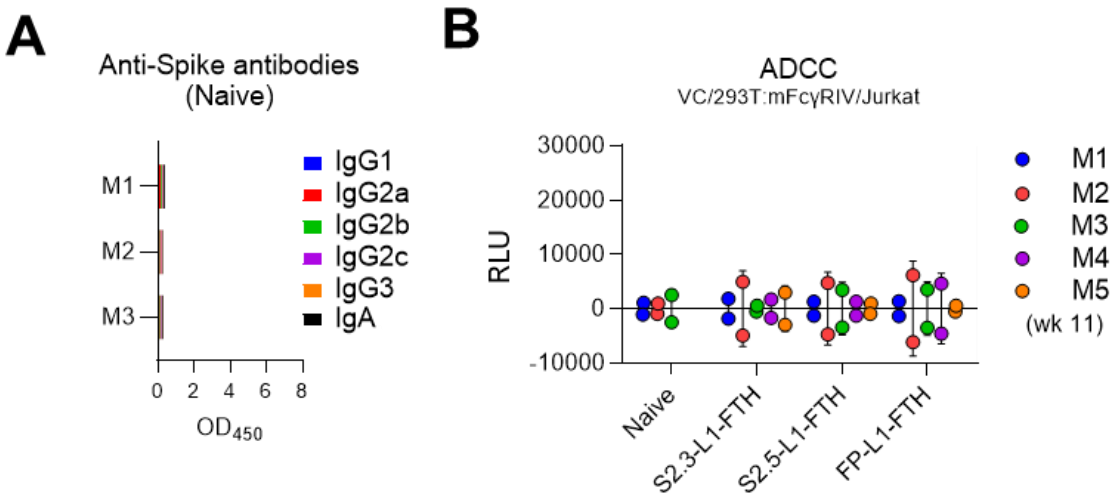

Figure S8. ADCC Activity of Antisera.

(A) IgG subclass distribution of spike-specific antibodies in naïve sera. Stacked bar graphs show the IgG subclass composition of spike-specific antibodies in naïve mice (n = 3), corresponding to the control data presented in Fig. 3G. **(B)** ADCC activity of antisera. HEK293T cells transfected with vector control were used as target cells and incubated with mouse immune sera, followed by the addition of FcγRIV/NFAT-Jurkat reporter cells as described for Fig. 3G. Each point represents serum from an individual immunized mouse (n = 5), with naïve sera (n = 3) included as controls.

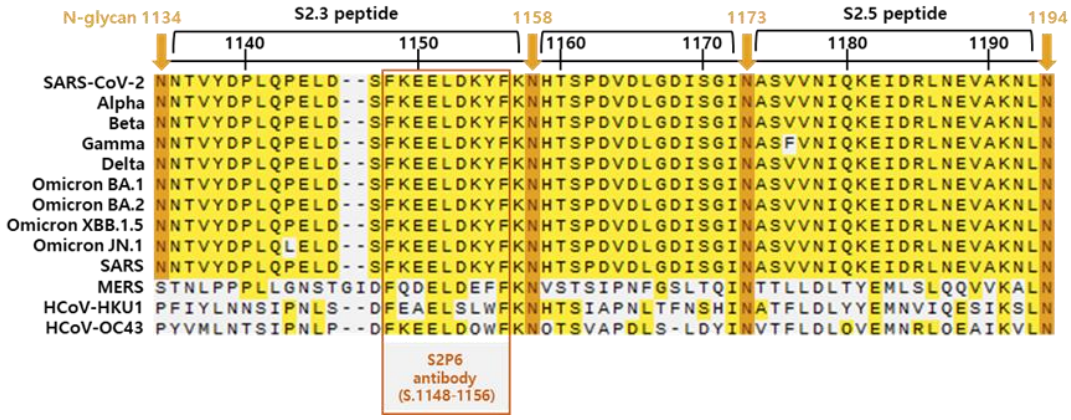

Figure S9. Sequence Alignment of the S2 Region Across SARS-CoV-2 Variants and Related β-Coronaviruses.

Sequence alignment of the S2 region from SARS-CoV-2 variants and related β-coronaviruses is shown. N-linked glycosylation sites are indicated in orange, and conserved residues are highlighted in yellow, illustrating the high degree of conservation within the S2 stem region across β-coronaviruses. The epitope recognized by the S2P6 antibody is indicated by a box.

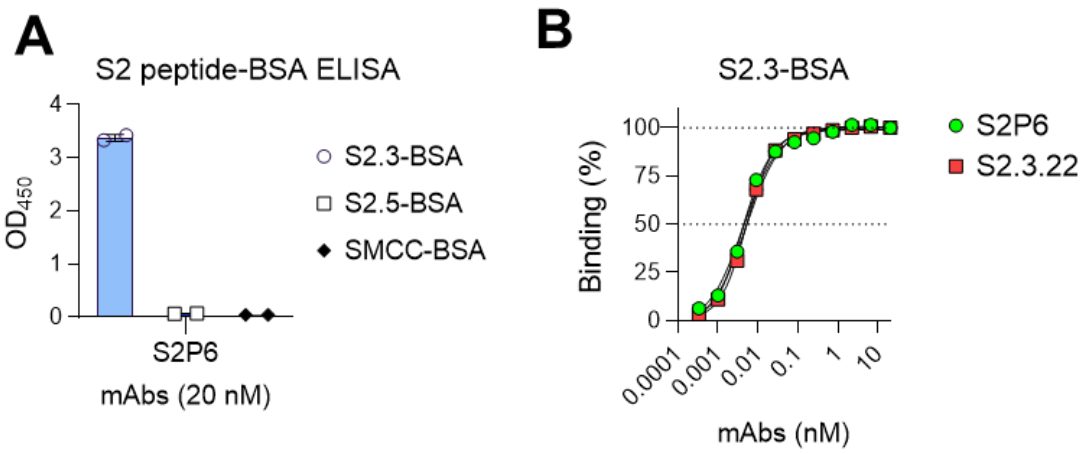

mAb clone	**EC50** ($x10^3$ nM)	Isotype/ Light chain
S2P6	4.55	Hu_IgG1/κ

Figure S10. Reactivity of the S2P6 Antibody to S2 Peptides.

(A) Reactivity of S2P6 antibody to S2.3 and S2.5 peptides. S2.3 or S2.5 peptides chemically conjugated to BSA were used as coating antigens to assess S2P6 binding by ELISA, with SMCC-treated BSA used as a negative control. **(B)** Titration analysis of S2P6 binding to the S2.3 peptide. Serially diluted S2P6 antibody was tested for binding to S2.3–BSA, and its binding activity was compared with that of the reference antibody S2.3.22, showing comparable apparent binding affinity. S2P6 is a human IgG1-type antibody with kappa light chain.

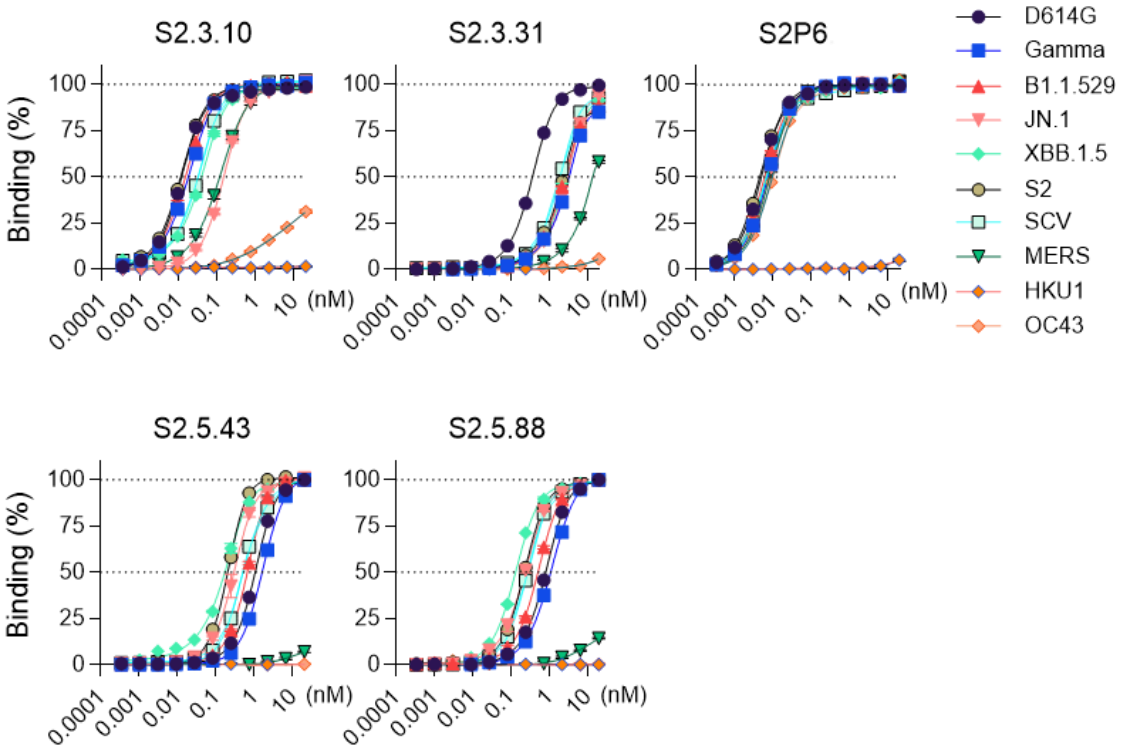

Figure S11. Titration Analysis of S2-Specific Monoclonal Antibodies.

Serially diluted S2-specific monoclonal antibodies were tested for binding to spike proteins from SARS-CoV-2 D614G, Gamma, Omicron sublineages, SARS-CoV, MERS-CoV, and seasonal HCoVs using the same ELISA setup as in Fig. 4D. EC_{50} values determined from these binding curves were used to generate the spot plots shown in Fig. 4D, and the complete set of EC_{50} values is summarized in Table S3.

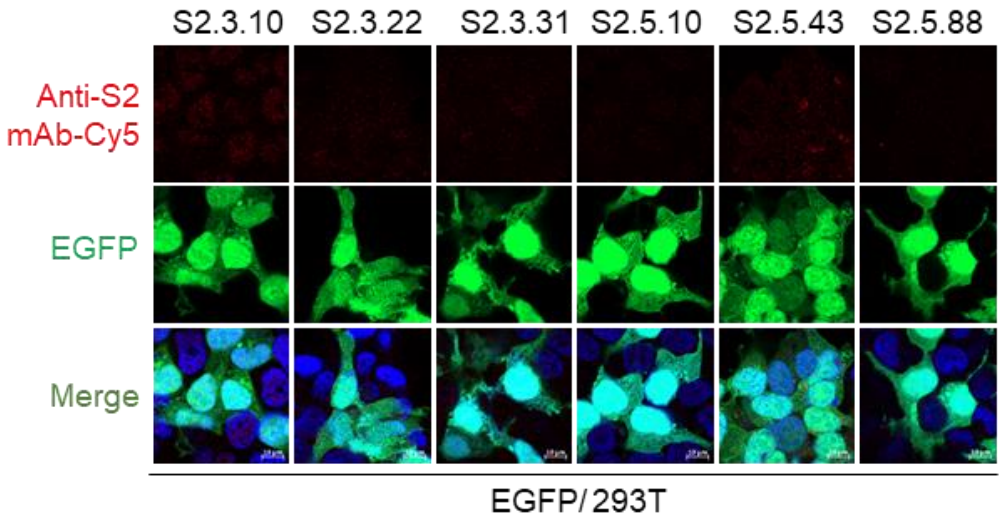

Figure S12. Immunofluorescence Analysis of Nonspecific Binding of S2 Antibodies in EGFP-Expressing HEK293T Cells.

HEK293T cells expressing EGFP were stained with S2 monoclonal antibodies, followed by Cy5-conjugated secondary antibodies, and analyzed by confocal microscopy to assess background nonspecific binding. This analysis corresponds to the control experiment shown in Fig. 4F.

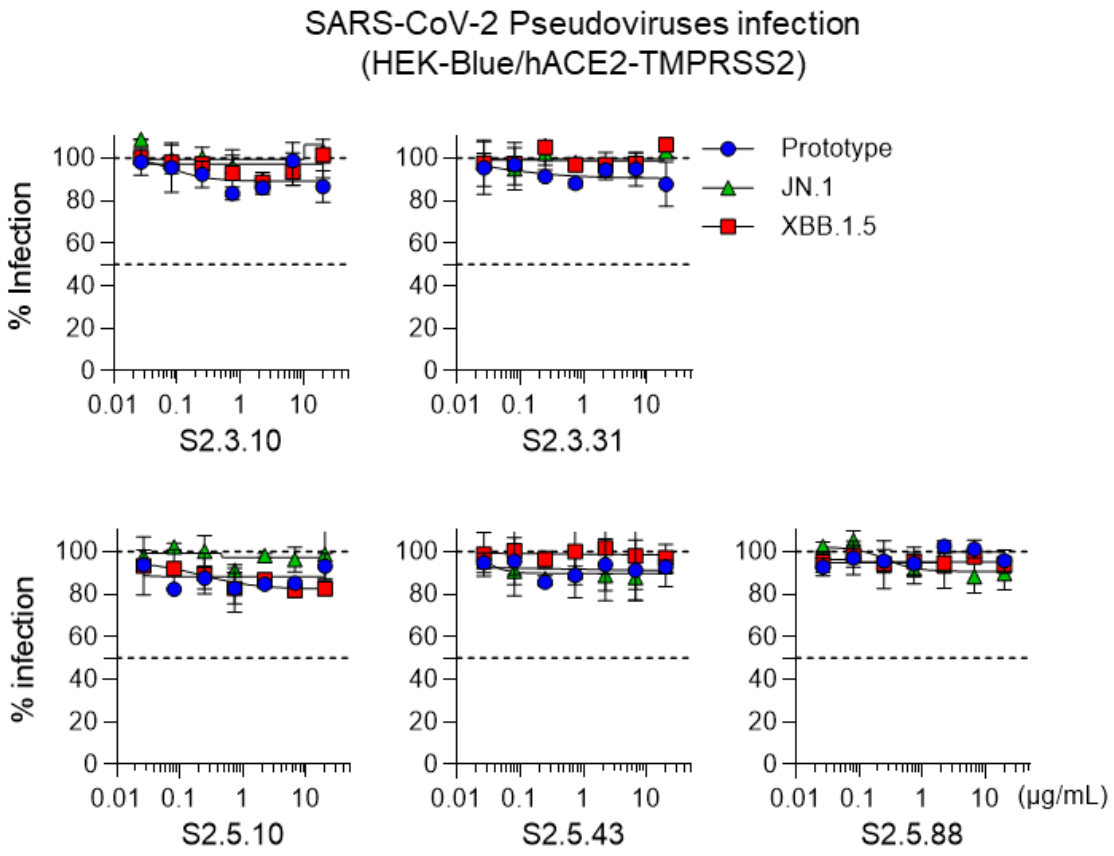

Figure S13. Pseudovirus Neutralization by S2-Specific Monoclonal Antibodies in TMPRSS2-Positive HEK-Blue/hACE2 Cells.

Pseudoviruses bearing SARS-CoV-2 prototype or Omicron variant spikes (XBB.1.5 and JN.1) were pre-incubated with serially diluted S2-specific monoclonal antibodies prior to infection of TMPRSS2-positive HEK-Blue/hACE2 cells. Neutralization was quantified by measuring reporter activity, with the signal from cells infected in the absence of antibody defined as 100% infection and relative infection levels in antibody-treated samples expressed as a percentage of this value.

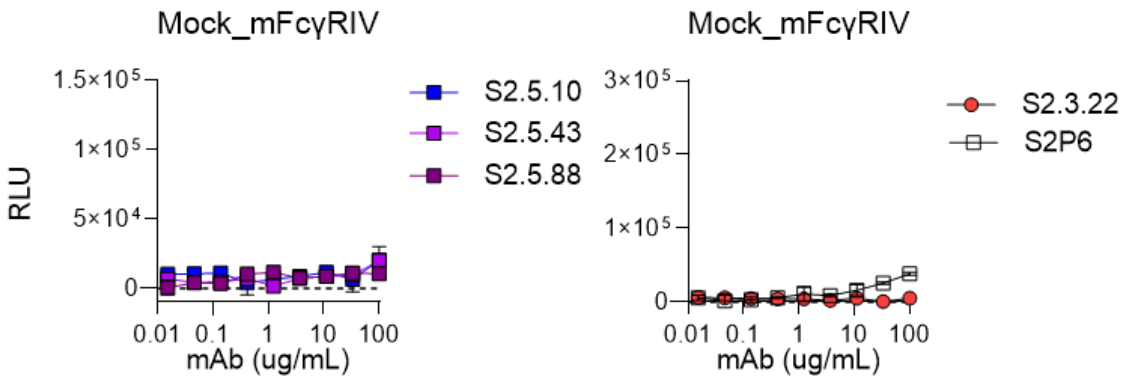

Figure S14. Antibody-Dependent Cellular Cytotoxicity (ADCC) Control Assay.

HEK293T cells expressing vector control were used as target cells and incubated with serially diluted monoclonal antibodies as a negative control for Fig. 5G. Mouse FcγRIV/NFAT-Jurkat reporter cells were added as effector cells under the same conditions as described for Fig. 5G. Fc-dependent effector activation was quantified by measuring luciferase activity, and results are shown as relative light units (RLU).

Table S1. SEC–MALS analysis of SC-FTH nanoparticles

	Peak 1	Peak 2	Peak 3
Masses*			
Injected Mass (µg)	0	0	0
Calculated Mass (µg)	4.58	31.34	172.84
Mass Recovery (%)	n/a	n/a	n/a
Mass Fraction (%)	2.2	15	82.8
Molar mass moments (g/mol)**			
Mn	1.008×10^7 (±0.371%)	1.901×10^6 (±0.237%)	8.374×10^5 (±0.161%)
Mp	1.128×10^7 (±0.404%)	1.862×10^6 (±0.237%)	8.404×10^5 (±0.107%)
Mv	n/a	n/a	n/a
Mw	1.103×10^7 (±0.404%)	1.916×10^6 (±0.234%)	8.383×10^5 (±0.158%)
Mz	1.216×10^7 (±0.938%)	1.934×10^6 (±0.520%)	8.392×10^5 (±0.352%)
Polydispersity			
Mw/Mn	1.093 (±0.549%)	1.008 (±0.333%)	1.001 (±0.226%)
Mz/Mn	1.206 (±1.009%)	1.017 (±0.572%)	1.002 (±0.387%)
rms radius moments (nm)			
Rn	32.6 (±1.4%)	13.8 (±5.0%)	7.4 (±11.7%)
Rw	33.6 (±1.4%)	13.9 (±4.9%)	7.4 (±11.7%)
Rz	34.9 (±1.3%)	13.9 (±4.8%)	7.4 (±11.6%)

*Injected mass indicates the total amount of sample loaded onto the column. Calculated mass represents the molecular weight (Mw) determined from light scattering signals. Mass fraction corresponds to the relative proportion of each eluting species.

**Molar mass moments (Mn, Mw, Mz) describe the molecular weight distribution within each peak. Polydispersity is defined as Mw/Mn.

Table S2. Immunoglobulin isotypes of S2-specific monoclonal antibodies.

mAb clone	Isotype/ Light chain
S2.3.10	IgG1/ κ
S2.3.22	IgG1/ κ
S2.3.31	IgG1/ κ
S2.5.10	IgG2a/ κ
S2.5.43	IgG2b/ κ
S2.5.88	IgG2b/ κ

Table S3. EC50 values of anti-S2 monoclonal antibodies for binding to SARS-CoV-2 spike antigens (ELISA)

Antigen	EC50 (nM)						
	S2P6	S2.3.10	S2.3.22	S2.3.31	S2.5.10	S2.5.43	S2.5.88
D614G	0.005	0.011	0.002	0.365	0.016	1.058	0.818
Gamma	0.007	0.018	0.002	2.715	0.007	1.656	1.148
B1.1.529	0.006	0.015	0.002	2.218	0.004	0.665	0.515
JN.1	0.008	0.146	0.002	2.848	0.007	0.294	0.231
XBB.1.5	0.007	0.039	0.002	2.560	0.006	0.172	0.132
S2	0.005	0.011	0.002	1.915	0.003	0.205	0.225
SCV	0.007	0.033	0.002	1.825	0.063	0.529	0.272
MERS	0.008	0.114	0.004	7.365	0.199	ND	ND
HKU1	ND*	ND	ND	ND	ND	ND	ND
OC43	0.010	> 10	0.866	> 10	ND	ND	ND

*ND: EC50 not determined.

Table S4. Kinetic analysis of anti-S2 monoclonal antibodies interacting with SARS-CoV-2 spike (D614G) by SPR

mAb	S2.3.22	S2.5.10	S2P6*
ka ($M^{-1}\cdot s^{-1}$)	2.482.E+05	3.469.E+05	8.936.E+05
kd (s^{-1})	8.049.E-05	1.382.E-03	4.478.E-04
KD (M)	3.242.E-10	3.984.E-09	5.01E-10
Rmax (RU)	26.24	7.264	28.1
Chi^2 (RU^2)	3.59	0.216	2.49
U-value	33	3	5

*The spike-binding affinity of S2P6 was obtained from previously reported studies (ref 33).